J. Chem. Sci. (2020) 132:43
https://doi.org/10.1007/s12039-020-1745-z

REGULAR ARTICLE

A reversible, benzothiazole-based "Turn-on" fluorescence sensor for selective detection of Zn^{2+} ions *in vitro*

DULAL MUSIB[a], MD KAUSAR RAZA[b], SALAM SUJATA DEVI[a] and MITHUN ROY[a,*]
[a]Department of Chemistry, National Institute of Technology Manipur, Langol, Imphal West, Manipur 795 004, India
[b]Department of Inorganic and Physical Chemistry, Indian Institute of Science, Bangalore, CV Raman Avenue, Bangalore, Karnataka 560 012, India
E-mail: mithunroy@nitmanipur.ac.in; mithunroy.iisc@gmail.com

MS received 20 November 2019; revised 8 December 2019; accepted 27 December 2019

Abstract. Temperature-driven, highly sensitive and selective "TURN-ON" fluorometric detection of Zn^{2+} by benzothiazole-based probes (L^1 and L^2) was reported in physiological pH in the present work. Iron(II) acted as the reversible switch or trigger for the reversible detection of Zn^{2+} ions by the probes resulting in "TURN-OFF" fluorescence at room temperature. However, selective detection of Zn^{2+} in the presence of Fe^{2+} was irreversible at 0–5 °C. Such temperature dependence on reversible fluorometric detection of Zn^{2+} in the presence of Fe^{2+} was explained from the thermodynamic perspective as well as DFT calculations in which the absolute enthalpy (H) and Gibbs free energy (G) of the resultant complexes and the fluorophores (L^1 and L^2) at different temperatures were determined. Enhanced fluorescence of the Zn^{2+} bound probes was due to the inhibition of excited-state intramolecular proton transfer (ESIPT). Effect of solvents, pH, and temperature on the fluorometric detection of Zn^{2+} was also probed in the present work. The results were translated into the visual detection of Zn^{2+} on paper-based fluorescence probe and later we demonstrated the sensing of mobile Zn^{2+} ions by the probes in living HeLa cells as the proof of concept of our present investigations.

Keywords. Reversible and selective detection of Zn^{2+}; Fe^{2+} as the reversible switch; pH and temperature dependence; DFT and TD-DFT; On-site screening analysis; Cellular imaging.

1. Introduction

Zinc and iron are the most abundant essential d-block elements and play several important roles in biological systems.[1] In most of the cases, zinc is coordinated to thiol-based proteins either as a catalytic cofactor or plays crucial structural role in several metalloenzymes,[2,3] except in the tissues of brain, pancreas, prostate, mammary gland where mobile zinc in the ion pools those are critically important in complex signaling processes like auditory processing and also in fertilization.[4–8] The permissible daily dietary intake of zinc for humans is about 8–11 mg.[9] Critically higher concentration of zinc than the permissible limit may suppress the uptake of essential elements like copper and iron.[10] Lower concentration of Zn^{2+} in the human body would result in several neurological disorders like Alzheimer's disease and diabetes.[11] Diarrhoea, immune dys function are the result of zinc deficiency in children under the age of five years.[12] Iron also plays a significant role in biology and critically low concentration of iron leads to several diseases like anaemia, liver and kidney damage, diabetes, and heart failure, etc.[13] Free, excess iron in biological system often result in undesirable generation of biologically toxic ROS.[14] Nonetheless, the importance of zinc and iron is underlying in the fact that more than 2 billion people are affected by deficiency of zinc (Zn) and iron (Fe) and account for almost two-thirds of the childhood deaths, particularly in under-developing countries, according to WHO.[15]

*For correspondence

Electronic supplementary material: The online version of this article (https://doi.org/10.1007/s12039-020-1745-z) contains supplementary material, which is available to authorized users.

Published online: 15 February 2020

Despite much research, the neurophysiological and neuropathological significance of mobile Zn(II) remains enigmatic. The lack of suitable probes for studying the role of mobile zinc or iron trafficking with the spatial-temporal resolution is extremely challenging. Fluorometric detection of metal ions, anions or small molecules (*e.g.* hydrogen sulfide, fluorides, phosphate, hydrogen etc) *in vitro* by using small molecules has emerged as the hot research topic in recent years. The design and development of small molecular "TURN-ON" luminescent probe for sensing ions or molecules *in vitro* is relatively rare and challenging (Table S1, Supplementary Information).[16–19] Several such probes exhibiting "TURN ON-TURN OFF" fluorescence in the presence of zinc are bulky in nature or have a low affinity towards zinc (Table S1, Supplementary Information).[20–25] In all the cited cases the group or molecule responsible for "TURN-OFF" fluorescent signal was either PPi or EDTA. Recently, the electronic and charge transfer property (ESIPT) of the benzothiazole moiety was investigated in detail probing the photo-physical importance of benzothiazole group of molecules in current research on diagnostics.[26,27]

In the present work, we have reported temperature-driven, tunable and highly sensitive fluorometric detection of mobile zinc *in vitro* by the benzothiazole-based fluorescent probes (L^1 and L^2) in which Fe^{2+} was used as the reversible switch for detection of Zn^{2+} (Scheme 1). The present work included the synthesis and characterization of the probes (L^1 and L^2), "TURN-ON" fluorometric detection of mobile zinc, studies on the binding of probes to Zn^{2+} and Fe^{2+} at a different temperature, pH and solvents. *In silico* studies to understand the thermodynamic perspective of binding of the probes to Zn^{2+} and Fe^{2+}, visual detection of Zn^{2+} on paper-based fluorescence probe and detection of mobile Zn^{2+} ions in living HeLa cells.

2. Experimental

2.1 *Materials and method*

All the reagents were purchased from Sigma-Aldrich (USA), SD-Fine chemicals (India), HI-MEDIA and used without further purification. Solvents were purified following a standard protocol and double distilled water was used to prepare aqueous buffer. A reported synthetic procedure was used to synthesize 2-(2-hydroxyphenyl) benzothiazole (L^1) and 2-(3,5-Di-tert-butyl -2-hydroxyphenyl) benzothiazole (L^2) with minor modification.[28]

Solid-phase FT-IR spectra were recorded in Perkin-Elmer UATR TWO FT-IR Spectrometer, UV-Visible and emission spectra were recorded in Perkin-Elmer UV/VIS spectrometer and HITACHI F-7000 Fluorescence spectrophotometer, respectively. Fluorescence lifetime measurements were carried out in Time-correlated single-photon-counting (TCSPC) spectrometer (Horiba Jobin Yovon) in which nanosecond laser of 375 nm was used as the excitation source and the data was analyzed by a bi-exponential fitting program using IBH DAS-6 decay analysis software. Molar conductivity measurements were done by using a EUTECH INSTRUMENT CON 510 (India) conductivity meter. NMR spectra were recorded on a Bruker Avance 400 (400 MHz) spectrometer, using $CDCl_3$ as solvent and tetramethylsilane (TMS) as an internal standard. Mass spectra (MS) were recorded with a Bruker Esquire 3000 Plus spectro-photometer (Bruker-Franzen Analytic GmbH, Bremen, Germany). All theoretical calculations on all the ligands and complexes were carried out using Gaussian 09 rev. A.02. The input files to Gaussian 09 were prepared with Gauss view 5.0.8. IUPAC names of all compounds were determined by using ChemDraw professional 15.

2.2 *Synthesis and characterization*

Synthesis of ligands (L^1, L^2)

The probes (L^1 and L^2) were synthesized according to the published protocol and characterized analytically and spectroscopically previously by ^1H and ^{13}C NMR, Q-TOF

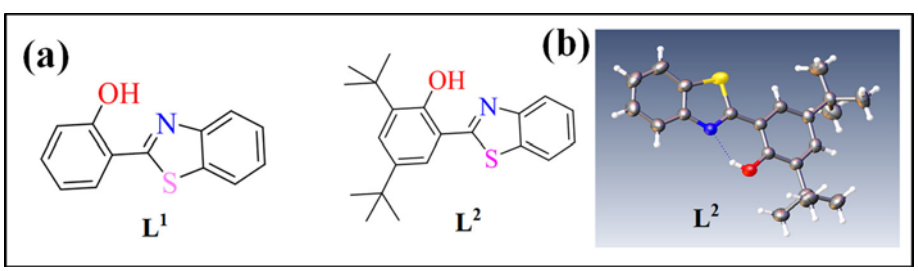

Scheme 1. (a) Schematic representation of the probes (L^1 and L^2). (b) ORTEP diagram of the probe, L^2 with 30% thermal ellipsoid parameter.

ESI MS, IR spectroscopy.[29] The probe L^2 was further characterized by single-crystal crystallography. The crystallographic information file was submitted to the Cambridge Crystallographic Data Centre (CCDC) (CCDC number: 1867449)

Selected X-ray crystallography information of L^2:

The light yellow colored rectangular shaped crystal of L^2 was grown from methanolic solution by slow evaporation. Empirical formula: $C_{21}H_{25}NOS$, Formula mass (g mol^{-1}) = 339.48, Crystal system = orthorhombic, space group = $Pna2_1$, a = 12.1085(5)Å, b = 9.6715(4)Å, c = 16.2332(6)Å, α(°) = 90,β(°) = 90, γ(°) = 90, V =1901.02(14)$Å^3$, Z = 4, F(000) = 728.0, GOOF = 1.035, [R1(Fσ> 2 2 σ) = R_1 = 0.0405, wR_2 = 0.1017,CCDC Number: 1867449.

3. Results and Discussion

3.1 *Synthesis, characterization and general aspects*

The fluorescent probes (L^1 and L^2) were synthesized by refluxing salicylaldehyde or 3,5-di-tertiary-2-hydroxybenzaldehyde and 2-aminophenol at 80 °C for 12 h in DMSO.[28] The reddish-yellow crude was purified by column chromatography by using 10% hexane and ethyl acetate as an eluent. Molecular structure of the probe L^1 was previously reported[29] and we have structurally characterized L^2 by single-crystal X-ray diffraction in the present work (Scheme 1, Figure S1–S2, CCDC number: 1867449).

3.2 *Photo-physical properties*

Benzothiazole-based probes (L^1 and L^2) have similar UV-visible spectrum in acetonitrile/HEPES buffer with very strong π-π* electronic transition at ∼285, 331 and 289, 346 nm (Table S2, Figure S3, Supplementary Information). However, π-π* transition for L^2 was red-shifted may be due to strong +I effect of bulky tertiary butyl group. The probes (L^1 and L^2) were emissive at 509 nm and 546 nm respectively in acetonitrile/HEPES buffer at 25 °C. The probes were photo-excited at 340 nm and 345 nm respectively to obtain the emission characteristics. Luminescent lifetime (τ) of the probes (L^1 and L^2) were determined to be 4.2 and 5.6 ns. The emissive properties of the probes were depended on the solvents. Non-polar solvents like hexane, benzene or dichloromethane had a significantly negative influence on the luminescent properties of the probes. Polar solvents like DMF, DMSO or aqueous DMSO (v/v 10% DMSO-H_2O) not only blue-shifted the emission but also intensified the emission (Figure S4, Supplementary Information). Likely, the significant pH dependence on the luminescent properties of the probes (L^1 and L^2) was observed. In the case of L^1, in acidic solution (pH < 6) the probe has shown strong luminescence at ∼460 nm, while in alkaline solution (pH > 8) the luminescence was red-shifted to 509 nm. The pKa value of L^1 is (neutral to monoanionic) 3.9.[30] The intense emission band at ∼460 nm may be assignable to the deprotonated phenolate anion of benzothiazole moiety whereas the emission at 509 nm is due to the protonated form benzothiazole ligand. A similar pH dependence of luminescence properties of the probe L^2 (λ_{em} = 546 nm) was not observed under similar experimental condition. The tunable luminescence behavior of L^2 was restricted due to the bulky tertiary butyl group (Figure S5, Supplementary Information). However, the optimized luminescence behavior of the probes at physiological pH 6–7 and biologically more benign aqueous DMSO (v/v 10% DMSO-H_2O) is of paramount importance for biological implications.

3.3 *"TURN-ON" fluorometric detection of mobile Zn^{2+}*

The luminescence spectra of the probes (L^1 and L^2) were recorded in acetonitrile/HEPES buffer solution (pH 7.2, 25 °C). Ligands L^1 and L^2 itself exhibits a week emission band at 509 nm (ϕ = 0.052) and at 546 nm (ϕ = 0.092), respectively due to the Excited-state Intramolecular Proton Transfer (ESIPT) and the sensing ability of the probes were determined in the presence of various metal ions including transition and non-transition metal ions (0.6 mM) (LiCl, KCl, NaCl, $CaCl_2$, $MgCl_2$, $BaCl_2$, $AlCl_3$, $MnCl_2$, $FeCl_2$, $FeCl_3$, $CoCl_2$, $NiCl_2$, $CuCl_2$, AgCl,$AuCl_3$, $ZnCl_2$, $CdCl_2$, $PbCl_2$, $HgCl_2$, $LaCl_3$, $AsCl_3$, $SnCl_2$, $PdCl_2$ and $PtCl_2$). Unlike other metal ions, Zn^{2+} had a remarkable influence on the fluorescence intensity of the probes (Figure 1, Figure S6, Supplementary Information). Addition of Zn^{2+} (0-0.6 mM) into the acetonitrile/HEPES buffer solution (pH 7.2, 25 °C) of L^1 and L^2 resulted in blue-shift of about 53 nm (L^1), 54 nm (L^2) with remarkable enhancement of fluorescence intensity may be due to the inhibition of the excited-state intramolecular proton transfer process of the probes (Figure 1, Figure S7, Supplementary Information). The limit of detection (LOD) of Zn^{2+} ion by L^1 was calculated to be 2.2 x 10^{-6}M and we compared the LOD value with the other previously reported Zn^{2+} sensing probes (Table S3, Figure S13, Supplementary Information).[31,32]

The luminescence quantum yield of the resultant complex was enhanced by 15-fold (Table S2,

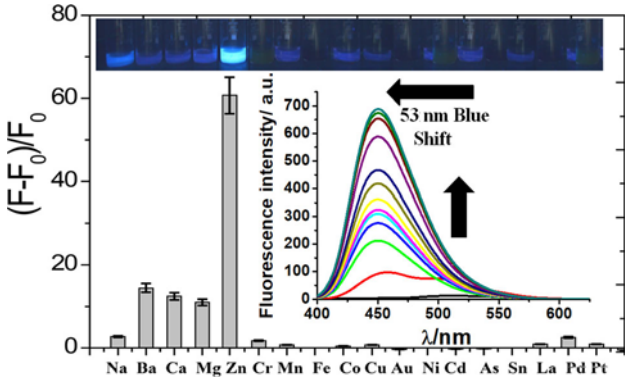

Figure 1. Graphical representation of the influence of different metal ions (0.6 mM) to the fluorescence of **L^1** in acetonitrile/HEPES buffer at 25 °C. The inset figure represents the fluorescence spectral (λ_{ex} = 340 nm) traces upon addition of increasing concentration of $ZnCl_2$ (0–0.6 mM) to 0.1 mM of **L^1** in acetonitrile/HEPES buffer at 25 °C.

Supplementary Information). Luminescence lifetime for the probes was determined to be 4.2 and 5.6 ns. We have, however, observed longer luminescence lifetime for the Zn^{2+} bound probes; 8.3 ns for L^1+Zn^{2+} and 9.98 ns for L^2+Zn^{2+} (Figure S8, Supplementary Information). Other metal ions (Li^+, Na^+, K^+, Ca^{2+}, Mg^{2+}, Ba^{2+}, Al^{3+}, Mn^{2+}, Fe^{2+}, Fe^{3+}, Co^{2+}, Ni^{2+}, Cu^{2+}, Ag^+, Au^{3+}, Cd^{2+}, Pb^{2+}, Hg^{2+}) had hardly any influence on the luminescence behavior of the probes L^1 and L^2 under the similar experimental condition. Such highly selective, "TURN-ON" fluorimetric Zn^{2+} sensing by the probes was remarkable in the tracking of mobile Zn^{2+} ions in biological samples.

Later we investigated the binding between the probes and Zn^{2+}, shown in Figure S9, Supplementary Information. Addition of Zn^{2+} ion (0–0.6 mM) led to gradually decrease in the absorption of ILCT bands [215 nm, 285 nm and 331 nm] for L^1, [221 nm, 289 nm and 346 nm] for L^2 and appearance of a new low intensity broad UV-visible band around 390 nm for L^1, 417 nm for L^2, which are assignable to the ligand to metal charge transfer transition, with isosbestic point at 358 nm (L^1), 371 nm (L^2). The structural aspects of the resultant complex formed on addition of Zn^{2+} into the acetonitrile/HEPES buffer solution (pH7.2) of L^1 and L^2 was determined from mass spectral analysis and Job's plot that revealed a 1:2 (Zn^{2+}:L) complex formation after the addition of Zn^{2+} into the solution of L^1 or L^2 (Figure S10–S12, Supplementary Information). Under such experimental condition, the binding constant for L^1 and L^2 with $Zn^{2+}$was determined to be 9.98 x $10^5 M^{-1}$ and 9.12 x 10^5 M^{-1} respectively which were significantly high. The 1:2 (Zn^{2+}:L^1) complex was previously confirmed by X-ray crystallography.[33]

Effect of pH on the binding of Zn^{2+} to L^1 was determined in acetonitrile/HEPES buffer solution with pH range 5.0–9.0 by fluorescence spectroscopy (Figure S14–S15, Supplementary Information). We observed optimized and highest binding affinity (K_b = 9.98 x 10^5 M^{-1}) of Zn^{2+} to the probe L^1 at a physiological pH of 7.2 at 25 °C. There was a reduced binding propensity of Zn^{2+} to L^1 either in acidic or alkaline pH. However, the binding affinity of Zn^{2+} to L^1 was responsible for remarkably enhanced luminescence intensity of the complex only at physiological pH which is of paramount importance in sensing Zn^{2+} in the biological sample by any synthetic probe.

Temperature influenced the fluorescence intensity of the Zn^{2+} bound probes in acetonitrile/HEPES buffer solution (pH 7.2) (Figure S16, Supplementary Information). We observed an inverse relationship of the luminescence intensity of Zn^{2+} bound probes. In fact, as the stability of the L^1+Zn^{2+} complex was increased in a lower temperature, the emission intensity of L^1+Zn^{2+} also enhanced. At higher temperature with reduced stability of L^1+Zn^{2+} complex, emission intensity was decreased. This deactivation was attributable to reduced stability of the resulted complex (L^1+Zn^{2+}) at higher temperature. However, the effect of UV-A light on the fluorescence behavior of L^1 was insignificant (Figure S16, Supplementary Information).

3.4 *Fe^{2+} as the switch for reversible detection of Zn^{2+}*

We discovered an interesting role of Fe^{2+} in fluorometric detection of Zn^{2+} by the probes (L^1 and L^2) in the present work. The role of Fe^{2+} is very important for the detection of Zn^{2+}. Unprecedently, iron (Fe^{2+}) acted as a reversible trigger or switch for sensing of Zn^{2+} ion by the probes. Although previously chelating ligand like pyrophosphate (PPI) or ethylenediaminetetraacetate (EDTA) was responsible "TURN-OFF" fluorescence any probe bound to Zn^{2+}.[34–36] The addition of 0.6 mM aqueous Zn^{2+} to the L^1 or L^2 significantly enhanced the emission of L^1 or L^2. However, on the addition of 0.45 mM aqueous solution Fe^{2+} to the highly emissive Zn^{2+} bound L^1 (L^1+Zn^{2+} or L^2+Zn^{2+}) solution resulted in the decrease in fluorescence almost to zero, with sufficiently low quenching rate. The addition of 0.6 mM aqueous solution of Zn^{2+} again maximized the emission (Figure 2, Figure S17–S18, Supplementary Information). Such "TURN ON-OFF-ON" luminescence behavior of L^1 upon addition of Zn^{2+} and Fe^{2+} ions were unprecedented in our present investigation.

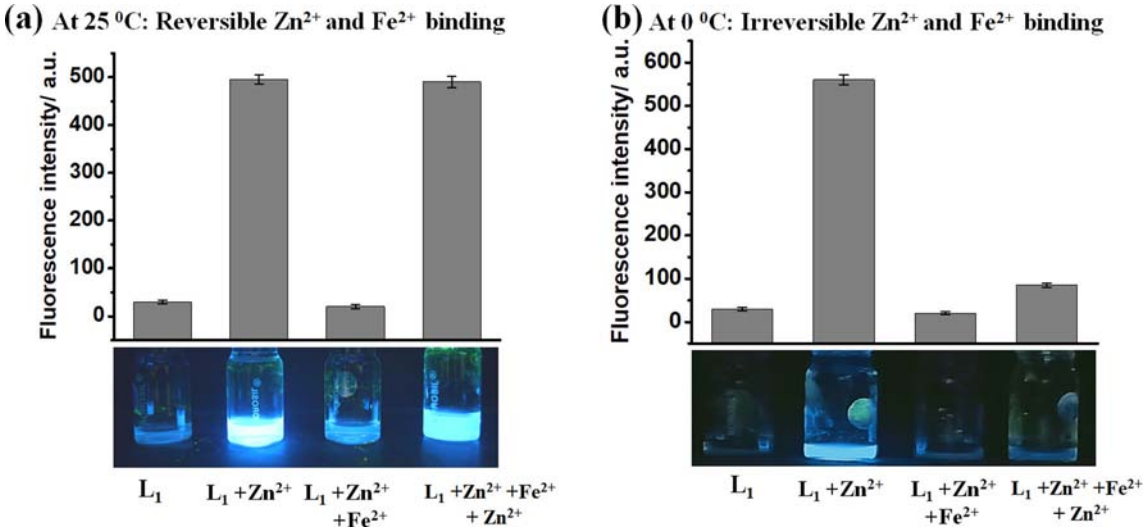

Figure 2. Temperature dependence on reversible fluorometric detection of Zn^{2+} (0.6 mM) in the presence of Fe^{2+} (0.45 mM) by the presence of the probes L^1. (a) at 25 °C and (b) at 0 °C.

In order to understand such reversibility, triggered by Fe^{2+} ion on luminescence behavior of L^1 bound to Zn^{2+}, we have studied the binding affinity of Zn^{2+} and Fe^{2+} to the probes in acetonitrile/HEPES buffer at 0 °C and at room temperature of 25 °C (Figure 2, Figure S19, Supplementary Information). Although the reversibility in luminescence behavior of the probes (L^1 and L^2) was remarkable at 25 °C, surprisingly we observed irreversible luminescence behavior of the probes at 0 °C. Although Fe^{2+} was able to quench the fluorescence of the Zn^{2+} bound probes, the addition of Zn^{2+} (1 mM) to the resultant solution resulted in hardly any enhancement in fluorescence intensity of the solution. Based on the observation we concluded that at 25 °C, the complex L^1+Zn^{2+} is thermodynamically unstable (also probed by the DFT calculations) and allowed ligand exchange on the addition of Fe^{2+} (0.45 mM) to form L^1+Fe^{2+} complex. The L^1+Fe^{2+} complex was also thermodynamically less stable at 25 °C and again resulted in ligand exchange reaction on the addition of Zn^{2+} (0.7 mM). The binding constant of L^1+Zn^{2+} and L^1+Fe^{2+} at 25 °C was determined to be 9.98 x 10^5 M^{-1} and 9.67 x 10^5 M^{-1}, which is are considerably comparable. However, the binding constant value determined for L^1+Fe^{2+} (1.12 x 10^6 M^{-1}) at 0 °C was significantly higher than that of the L^1+Zn^{2+} (9.36 x 10^6 M^{-1}), explaining the irreversibility in the detection of Zn^{2+} by the probe at a lower temperature. The proposed hypothesis was verified by mass spectral analysis (Figure S20–S21, Supplementary Information). Similar luminescence behavior was observed for the probe L^2. None the less, the binding of Zn^{2+} and Fe^{2+} to the probes has resulted in a thermodynamically less stable complex with the probes at room temperature leading to reversible, "TURN ON-OFF-ON" luminescence behavior of the probes in sensing Zn^{2+} in the presence of Fe^{2+} ions. However, at lower temperature Fe^{2+} binds the probes strongly leading to thermodynamically more stable L+Fe^{2+} complex and Zn^{2+} was unable to replace Fe^{2+}. With the rise in temperature, the ligand exchange reaction was facilitated with a steady enhancement of fluorescence intensity.

The reversibility in the detection of Zn^{2+} by the probe was confirmed by fluorescence spectrometry in which L^1 (0.10 mM) was added with first Fe^{2+} (0.45 mM) with negligible fluorescence. Addition of Zn^{2+} (0.70 mM) to the mixture again resulted in remarkable enhancement of fluorescence at room temperature. This confirmed reversibility of fluorimetric detection of Zn^{2+} in the presence of Fe^{2+} (Figure S22, Supplementary Information).

3.5 *DFT calculations*

We carried out DFT calculation not only to optimize the structures (Figure S23–S24, Supplementary Information) of the probes and the resultant complexes (L^1+Zn^{2+} and L^1+Fe^{2+}) at their respective ground state but also to have insight into the energetics (thermochemistry) of the probes and the complexes with Zn^{2+} and Fe^{2+} at 25 °C and 0 °C.[37–39] The structure of the complexes was proposed based on the mass spectral analysis. DFT calculations were performed by employing the DFT B3LYP/GEN level by using 6-31G(d,p) basis set for H, C, N, O, S atoms and LANL2DZ basis set for Zn^{2+}, Fe^{2+} atom in the gas

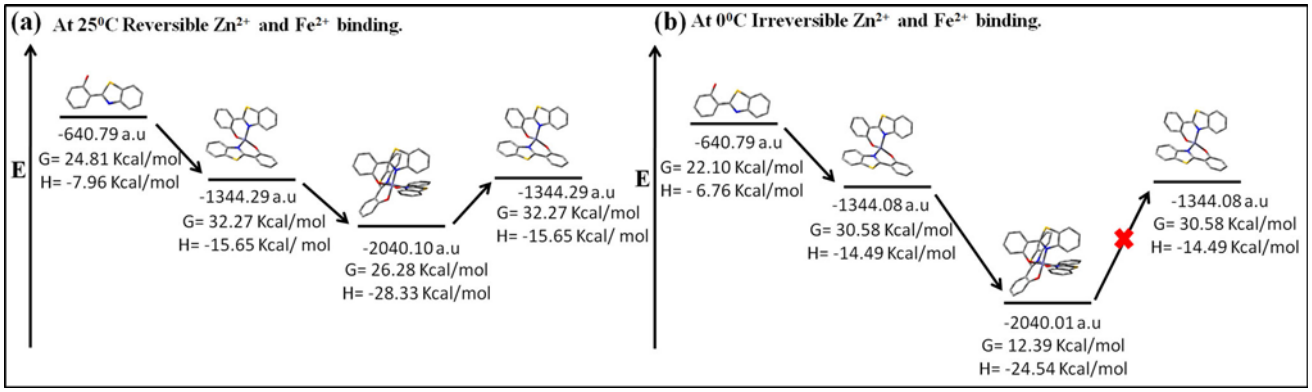

Figure 3. Optimized energy of the ligand ($\mathbf{L^1}$), Zinc complex ($\mathbf{L^1+Zn^{2+}}$) and Fe complex ($\mathbf{L^1+ Fe^{2+}}$) (a) at 25 °C and (b) at 0 °C calculated at the B3LYP/GEN level by using 6-31G(d,p) basis set for H, C, N,O,S atoms and LANL2DZ basic set for $\mathbf{Zn^{2+}}$, $\mathbf{Fe^{2+}}$ atom in the gas phase. Gibbs free energy and Enthalpy calculated through frequency calculation at freq = noraman ucam-b3lyp/lanl2dz/def2tzv geom = connectivity temperature = 298/273 k basis set. The energy scale (E) in the figure is qualitative.

phase. Excited-state chemistry and thermochemistry proved by TD-DFT and frequency calculation using UCAM-B3LYP/LANL2DZ/DEF2TZV basis set (Figure S25, Supplementary Information). Absolute enthalpy, the Gibbs free energy and binding constant (Logk) of L^1, L^1+Zn^{2+}, L^1+Fe^{2+} complexes, calculated at 0 °C and 25 °C, are given in Table S4, Supplementary Information. The difference in Gibb's free energy (ΔG^* = -5.304 Kcal/mol) of L^1+Zn^{2+} and L^1+Fe^{2+} conjugates at 25 °C was comparatively low which justified the ligand exchange at 25 °C and addition of Zn^{2+} again enhanced the fluorescence by forming L^1+Zn^{2+} species. However, at low-temperature (0 °C) energy barrier between the complexes L^1+Fe^{2+} and L^1+Zn^{2+} (ΔG^* = -17.601 Kcal/mol) is relatively high to make the system irreversible in luminescence response of the probe L^1 (Figure 3).

3.6 *On-site screening analysis*

Based on the results we developed a paper-based fluorescent sensor for visual detection of Zn^{2+} and to probe "TURN ON-OFF-ON" fluorescence behavior of the probe (L^1) in the presence of Zn^{2+} and Fe^{2+} metal ions. A 10 μM solution of L^1 in acetonitrile was carefully dropped onto filter paper strips and dried. Each spot gave the very pale blue (L^1) fluorescence when illuminated under UV-A light. Subsequent addition of a drop of 0.1 mM solution of various metal ions to the spots did not result in a significant change in the fluorescence of the probes except zinc (Figure 4, Figure S26, Supplementary Information). Similar "TURN ON-OFF-ON" fluorescence behavior of the probe (L^1) in the presence of Zn^{2+} and Fe^{2+} metal ions were also probed in paper strips signifying real-life application of the paper-based fluorescence sensor in detecting mobile Zn^{2+} in the analytes.

3.7 *Cellular uptake and detection of Zn^{2+} in vitro*

The ability of L^1 and L^2 to track and detect mobile Zn^{2+} ions in living HeLa cells was also examined by confocal microscopy. Initially, HeLa cells, incubated with 10 μM of L^1 and L^2 (2% DMSO-H_2O) for 15 min at 37 °C and was observed with a weak intracellular typical blue fluorescence indicating cytosolic localization of the probes in HeLa cells. Subsequent addition of 50 μM $ZnCl_2$ into the live HeLa cells, resulted in a remarkable visual change in fluorescence into intense bluish-green colour, exemplifying "TURN-ON" detection of Zn^{2+}*in vitro*. However, subsequent addition of 50 μM $FeCl_2$ resulted in "TURN-OFF" fluorescence in HeLa cells (Figure 5).[40–43]

4. Conclusions

The benzothiazole-based luminescent probes (L^1 and L^2) were developed for reversible and selective detection of mobile Zn^{2+} ions in live HeLa cells. Detection of Zn^{2+} by the probed resulted in "TURN ON" luminescence and Fe^{2+} acted as the reversible switch resulting in "TURN-OFF" luminescence response. However, the reversible luminescence behavior was temperature-dependent in which the reversibility in Zn^{2+} ion detection was observed only at room temperature or higher and become irreversible at 0–5 °C. This was rigorously explained by the DFT

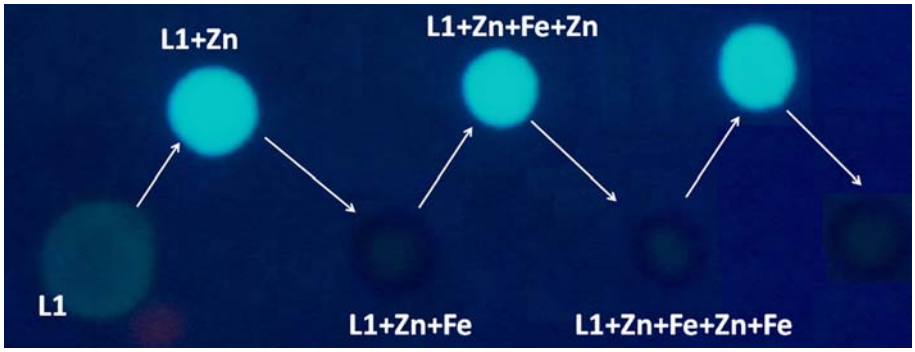

Figure 4. Photographic image of reversible detection Zn^{2+} metal ion by L^1 in the presence of Fe^{2+} on paper strip tested (λ_{ex} = 365 nm) at 25 °C.

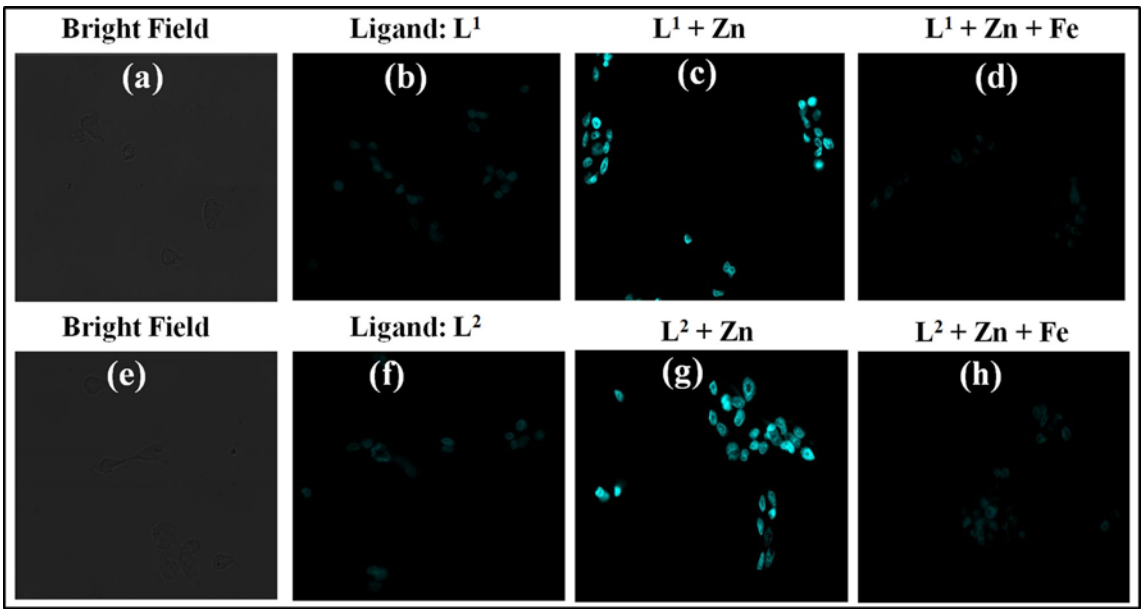

Figure 5. Live-cell imaging of HeLa cells after incubation with L^1 (10 μM) and L^2 (10 μM). (a) Bright-field transmission image. (b) Fluorescence image of L^1. (c) Fluorescence image of cells incubated with 50 μM $ZnCl_2$; Image was captured after 20 min. (d) Fluorescence images of cells incubated with 50 μM $FeCl_2$, Image captured after 10 min. (e) Bright-field transmission image. (f) Fluorescence image of L^2. (g) Fluorescence image of cells incubated with 50 μM $ZnCl_2$; Image captured after 20 min. (h) Fluorescence images of cells incubated with 50 μM $FeCl_2$, Image captured after 10 min.

calculations. We demonstrated reversible detection of Zn^{2+} in live HeLa cells and were able to develop a paper-based fluorescent sensor for on-site visual screening analysis. However, the probes (L^1 and L^2) were unable to detect Zn^{2+} in the ion pools containing Fe^{2+}. Fe^{2+} ion was observed to be antagonist to Zn^{2+} and irreversibly bind to the probes, making the probes inefficient in detecting Zn^{2+}. This was the critical observation in our present studies (Figure S27, Supplementary Information). Overall, sensitive detection of Zn^{2+} *in vitro* and on-site paper-based screening analysis by the probes, thorough understanding of kinetic/thermodynamics of Zn^{2+} sensing is of paramount importance in academic research as well as technology innovation.

Supplementary Information (SI)

Details on materials and experimental methods, DFT calculations, biological assay, ^1H and ^{13}C NMR, mass spectra, UV-visible and fluorescence spectra of the probes in the presence of Zn^{2+} and Fe^{2+}, Kinetic plots are available at www.ias.ac.in/chemsci.

Acknowledgements

We thank the Science and Engineering Research Board, Government of India, New Delhi for financial support [ECR-2016-000839/CS] and Board of Research in Nuclear Science (BRNS), Mumbai (37(2)/14/18/2017-BRNS) for financial support. We thank NIT Manipur for providing infrastructure. We sincerely thank Prof. Akhil R. Chakravarty, IISc

Bangalore for providing the facility of cellular studies. We thank Prof. Mohammad Qureshi, Central Instruments Facility (CIF), IIT Guwahati for measuring luminescent decay for the ligands and in presence of metals. We also thank Advanced Material Research Center, IIT Mandi for recording the ^{1}H and ^{13}C NMR, ESI mass spectra of the probes and the complexes.

References

1. Kleczkowski M and Garncarz M 2012 The role of metal ions in biological oxidation – the past and the present *Pol. J. Vet. Sci.* **15** 165
2. Zastrow M L and Pecoraro V L 2014 Designing Hydrolytic Zinc Metalloenzymes *Biochemistry* **53** 957
3. Laitaoja M, Valjakka J and Jänis J 2013 Zinc Coordination Spheres in Protein Structures *Inorg. Chem.* **52** 10983
4. Kelleher S L, Seo Y A and Lopez V 2009 Mammary gland zinc metabolism: regulation and dysregulation *Genes Nutr.* **4** 83
5. (a) Li L, Wang Y, Lei B, Han S, Yang Z, Poeppelmeier K R and Pan S 2016 A New Deep-ultraviolet Transparent Orthophosphate $LiCs_2PO_4$ with Large Second Harmonic Generation Response *J. Am. Chem. Soc.* **138** 9101; (b) Crivat G, Kikuchi K, Nagano T, Priel T, Hershfinkel M, Sekler I, Rosenzweig N and Rosenzweig Z 2006 Fluorescence-Based Zinc Ion Sensor for Zinc Ion Release from Pancreatic Cells *Anal. Chem.* **78** 5799
6. Bush A I, Pettingel W H, Multhaup G, Paradis M D, Vonsattel J, Gusella J F, Beyreuther K, Masters C L and Tanzi R E 1994 Rapid induction of Alzheimer A beta amyloid formation by zinc *Science* **265** 1464
7. (a) Goldberg J M, Wang F, Sessler C D, Vogler N W, Zhang D Y, Loucks W H, Tzounopoulos T and Lippard S J 2018 Photoactivatable Sensors for Detecting Mobile Zinc *J. Am. Chem. Soc.* **140** 2020; (b) Walkup G K, Burdette S C, Lippard S J and Tsien R Y 2000 A New Cell-Permeable Fluorescent Probe for Zn^{2+} *J. Am. Chem. Soc.* **122** 5644
8. (a) Goldsmith C R and Lippard S J 2006 Analogues of Zinpyr-1 Provide Insight into the Mechanism of Zinc Sensing *Inorg. Chem.* **45** 6474; (b) Chen C, Wang X, Li L, Huang Y and Cao R 2018 Highly selective sensing of Fe^{3+} by an anionic metal–organic framework containing uncoordinated nitrogen and carboxylate oxygen sites *Dalton Trans.* **47** 3452
9. (a) Prasad A S 1995 Zinc: an overview *Nutrition* **11** 93; (b) Roohani N, Hurrell R, Kelishadi R and Schulin R 2013 Zinc and its importance for human health: An integrative review *J. Res. Med. Sci.* **18** 144
10. (a) Heng S, Reineck P, Vidanapathirana A K, Pullen B J, Drumm D W, Ritter L J, Schwarz N, Bonder C S, Psalti P J, Thompson J G, Gibson B C, Nicholls S J and Abell A D 2017 Rationally Designed Probe for Reversible Sensing of Zinc and Application in Cells *ACS Omega* **2** 6201; (b) Ding A, Tang F, Wang T, Tao X and Yang J 2015 A α-cyanostilbene-modified Schiff base as efficient turn-on fluorescent chemosensor for Zn^{2+} *J. Chem. Sci.* **127** 375
11. (a) Hirano T, Kikuchi K, Urano Y and Nagano T 2002 Improvement and Biological Applications of Fluorescent Probes for Zinc, ZnAFs *J. Am. Chem. Soc.* **124** 6555; (b) Yu F, Guo X, Tian X and Jia L 2017 A Ratiomeric Fluorescent Sensor for Zn^{2+} Based on N,N′-Di(quinolin-8-yl)oxalamide *J. Fluoresc.* **27** 723
12. Kim J H, Hwang I H, Jang S P, Kang J, Kim S, Noh I, Kim Y, Kim C and Harrison R G 2013 Zinc sensors with lower binding affinities for cellular imaging *Dalton Trans.* **42** 5500
13. (a) Eid R, Arab N T T and Greenwood M T 2017 Iron mediated toxicity and programmed cell death: A review and a re-examination of existing paradigms *BBA-Mol. Cell. Res.* **1864** 399; (b) Gernand A D, Schulze K J, Stewart C P, West Jr. K P and Christian P 2016 Micronutrient deficiencies in pregnancy worldwide: health effects and prevention *Nat. Rev. Endocrinol.* **12** 274
14. Tsonev T and Lidon F J C 2012 Zinc in plants - An overview *Emir. J. Food Agric.* **24** 322
15. (a) Liu H, Venkatesan P and Wu S 2014 A sensitive and selective fluorescent sensor for Zinc(II) and its application to living cell imaging *Sens. Actuat. B Chem.* **203** 719; (b) Su P, Zhu Z, Wang J, Cheng B, Wu W, Iqbal K and Tang Y 2018 A biomolecule-based fluorescence chemosensor for sequential detection of Ag^{+} and H_2S in 100% aqueous solution and living cells *Sens. Actuat. B Chem.* **273** 93
16. (a) You Y, Lee S, Kim T, Ohkubo K, Chae W, Fukuzumi S, Jhon G, Nam W and Lippard S J 2011 Phosphorescent Sensor for Biological Mobile Zinc *J. Am. Chem. Soc.* **133** 18328; (b) Meeusen J W, Nowakowski A and Petering D H 2012 Reaction of Metal-Binding Ligands with the Zinc Proteome: Zinc Sensors and N,N,N′,N′-Tetrakis(2-pyridylmethyl)-ethylenediamine *Inorg. Chem.* **51** 3625
17. (a) Saha U C, Chattopadhyay B, Dhara K, Mandal S K, Sarkar S, Khuda-Bukhsh A R, Mukherjee M, Helliwell M and Chattopadhyay P 2011 A Highly Selective Fluorescent Chemosensor for Zinc Ion and Imaging Application in Living Cells *Inorg. Chem.* **50** 1213; (b) Tang L, Wu D, Huang Z and Bian Y 2016 A fluorescent sensor based on binaphthol-quinoline Schiff base for relay recognition of Zn^{2+} and oxalate in aqueous media *J. Chem. Sci.* **128** 1337
18. (a) Nolan E M, Jaworski J, Racine M E, Sheng M and Lippard S J 2006 Midrange Affinity Fluorescent Zn(II) Sensors of the Zinpyr Family: Syntheses, Characterization, and Biological Imaging Applications *Inorg. Chem.* **45** 9748; (b) Chabosseau P, Woodier J, Cheung R and Rutter G A 2018 Sensors for measuring subcellular zinc pools *Metallomics* **10** 229
19. Nowakowski A B, Meeusen J W, Menden H, Tomasiewicz H and Petering D H 2015 Chemical−Biological Properties of Zinc Sensors TSQ and Zinquin: Formation of Sensor-Zn-Protein Adducts versus $Zn(Sensor)^2$ Complexes *Inorg. Chem.* **54** 11637
20. (a) Ingale S A and Seela F 2012 A Ratiometric Fluorescent On−Off Zn^{2+} Chemosensor Based on a Tripropargylamine Pyrene Azide Click Adduct *J. Org. Chem.* **20** 9352; (b) Hirano T, Kikuchi K, Urano Y, Higuchi T and Nagano T 2000 Highly Zinc-Selective

Fluorescent Sensor Molecules Suitable for Biological Applications *J. Am. Chem. Soc*. **122** 12399
21. (a) Li M, Lu H, Liu R, Chen J and Chen C 2012 Turn-On Fluorescent Sensor for Selective Detection of Zn^{2+}, Cd^{2+}, and Hg^{2+} in Water *J. Org. Chem*. **77** 3670; (b) Qin J, Fan L, Yang Z 2016 A small-molecule and resumable two-photon fluorescent probe for Zn^{2+} based on a coumarin Schiff-base *Sens. Actuat. B Chem.* **228** 156
22. Yan X, Kim J J, Jeong H S, Moon Y K, Cho Y K, Ahn S, Jun S B, Kim H and You Y 2017 Low-Affinity Zinc Sensor Showing Fluorescence Responses with Minimal Artifacts *Inorg. Chem.* **56** 4332
23. Yang Y, Ma C, Zhang Y, Xue Q, Ru J, Liu X and Guo H 2018 A highly selective "turn-on" fluorescent sensor for zinc ion based on a cinnamylpyrazoline derivative and its imaging in live cells *Anal. Methods* **10** 1833
24. Mawai K, Nathani S, Roy P, Singh U P and Ghosh K 2018 Combined experimental and theoretical studies on selective sensing of zinc and pyrophosphate ions by rational design of compartmental chemosensor probe: Dual sensing behaviour via secondary recognition approach and cell imaging studies *Dalton Trans*. **47** 6421
25. Shyamal M, Mazumdar P, Maity S, Samanta S, Sahoo G P and Misra A 2016 Highly Selective Turn-On Fluorogenic Chemosensor for Robust Quantification of Zn(II) Based on Aggregation Induced Emission Enhancement Feature *ACS Sens*. **6** 739
26. (a) Lee J, Kim C H and Joo T 2013 Active role of proton in excited state intramolecular proton transfer reaction *J. Phys. Chem. A* **117** 1400; (b) Gangopadhyay A, Ali S S, Guria U N, Samanta S K, Sarkar R, Datta P and Mahapatra A K 2018 A ratiometric hypochlorite sensor guided by PET controlled ESIPT output with real time application in commercial bleach *New J. Chem.* **42** 15990
27. (a) Kungwan N, Plassser F, Aquino A J A, Barbatti M, Wolschann P and Lischka H 2012 The effect of hydrogen bonding on the excited-state proton transfer in 2-(2′-hydroxyphenyl)benzothiazole: a TDDFT molecular dynamics study *Phys. Chem. Chem. Phys*. **14** 9016; (b) Karmakar P, Manna S, Ali S S, Guria U N, Sarkar R, Datta P, Mandal D and Mahapatra A K 2018 Reaction-based ratiometric fluorescent probe for selective recognition of sulfide anions with a large Stokes shift through switching on ESIPT *New J. Chem.* **42** 76
28. (a) Warde U and Sekar N 2017 Comprehensive study on Excited State Intramolecular Proton Transfer in 2-(benzo[d]thiazol-2-yl)-3-methoxynaphthalen-1-ol and 2-(benzo[d]thiazol-2-yl)naphthalene-1,3-diol: Effect of solvent, aggregation, viscosity and TDDFT study *J. Photochem. Photobiol.* **337** 33; (b) www.ccdc.cam.ac.uk (CCDC number: 133836)
29. (a) Musib D, Raza M K, Martina K and Roy M 2019 Mn(I)-based photo CORMs for trackable, visible light-induced CO release and photocytotoxicity to cancer cells *Polyhydron* **172** 125; (b) Musib D, Banerjee S, Garai A, Soraisam U and Roy M 2018 Synthesis, Theory and In Vitro Photodynamic Activities of New Copper(II)-Histidinito Complexes *Chemistry Select* **3** 2767
30. Bardajee G R, Mohammadi M and Kakavand N 2016 Copper(II)–diaminosarcophagine-functionalized SBA-15: a heterogeneous nanocatalyst for the synthesis of benzimidazole, benzoxazole and benzothiazole derivatives under solvent-free conditions *Appl. Organomet. Chem.* 30 51
31. (a) Sohrabi M, Amirnasr M, Meghdadi S, Lutz M, Torbati B M and Arrokhpour F H 2018 A highly selective fluorescence turn-on chemosensor for Zn^{2+}, and its application in live cell imaging, and as a colorimetric sensor for Co^{2+}: experimental and TD-DFT calculations *New J. Chem.* **42** 12595; (b) Vongnam K, Aree T, Sukwattanasinitt M and Rashatasakhon P 2018 Aminoquinoline-Salicylaldimine Dyads as Highly Selective Turn-On Fluorescent Sensors for Zinc (II) Ions *Chem. Select* **3** 3495; (c) Yang Y, Ma C, Zhang Y, Xue Q, Ru J, Liu X and Guo H 2018 A highly selective "turn-on" fluorescent sensor for zinc ion based on a cinnamyl pyrazoline derivative and its imaging in live cells *Anal. Methods* **10** 1833
32. (a) Chang C, Wang F, Wei T and Chen X 2017 Benzothiazole-based fluorescent sensor for ratiometric detection of Zn(II) ion and secondary sensing PPi and its applications for biological imaging and PPase catalysis assays *Ind. Eng. Chem. Res.* **56** 8797; (b) Vishaka V H, Saxena M, Balakrishna R G, Latiyan S and Jain S 2019 Remarkably selective biocompatible turn-on fluorescent probe for detection of Fe^{3+} in human blood samples and cells *RSC Adv.* **9** 27439; (c) Cao X, Zhang F, Bai Y, Ding X and Sun W 2019 A Highly Selective BTurn-on^ Fluorescent Probe for Detection of Fe^{3+} in Cells *J. Fluoresc.* **29** 425
33. Yu G, Yin S, Liu Y, Shuai Z and Zhu D 2003 Structures, Electronic States, and Electroluminescent Properties of a Zinc(II) 2-(2-Hydroxyphenyl)benzothiazolate Complex *J. Am. Chem. Soc*. **125** 14816
34. Zastrow M L, Radford R J, Chyan W, Anderson C T, Zhang D Y, Loas A, Tzounopoulos T and Lippard S J 2016 Reaction-Based Probes for Imaging Mobile Zinc in Live Cells and Tissues *ACS Sens.* **1** 32
35. Boonkitpatarakul K, Wang J, Niamnont N N, Liu B, Mcdonald L, Pang Y and Sukwattanasinitt M 2016 Novel Turn-On Fluorescent Sensors with Mega Stokes Shifts for Dual Detection of Al^{3+} and Zn^{2+} *ACS Sens.* **1** 144
36. Lohar S, Pal S, Mukherjee M, Maji A, Demitri N and Chattopadhyay P 2017 A turn-on green channel Zn^{2+} sensor and the resulting zinc(II) complex as a red channel HPO_4^{2-} ion sensor: a new approach *RSC Adv*. **7** 25528
37. (a) Trucks W G, Schlegel B H, Scuseria E G, Robb A M, Cheeseman R J, Scalmani G, Barone V, Mennucci B, Petersson A G, Nakatsuji H, Caricato M, Li X, Hratchian P H, Izmaylov F A, Bloino J, Zheng G, Sonnenberg L J, Hada M, Ehara M, Toyota K, Fukuda R, Hasegawa J, Ishida M, Nakajima T, Honda Y, Kitao O, Nakai H, Vreven T, Montgomery A J, Peralta E J, Ogliaro F, Bearpark M, Heyd J J, Brothers E, Kudin N K, Staroverov V N, Keith T, Kobayashi R, Normand J, Raghavachari K, Rendell A, Burant C J, Iyengar S S, Tomasi J, Cossi M, Rega N, Millam M J, Klene M, Knox E J, Cross B J, Bakken V, Adamo C, Jaramillo J, Gomperts R, Stratmann E R, Yazyev O, Austin J A, Cammi R, Pomelli C, Ochterski W J, Martin L R, Morokuma K, Zakrzewski G V, Voth A G, Salvador P, Dannenberg J J, Dapprich S,

Daniels D A, Farkas O, Foresman B J, Ortiz V J, Cioslowski J and Fox J D 2013 Gaussian, Inc., Gaussian 09, Revision, D.01, M. J. Frisch, Wallingford CT; (b) http://gaussian.com/thermo/

38. (a) Dreuw A and Head-Gordon M 2004 Failure of Time-Dependent Density Functional Theory for Long-Range Charge-Transfer Excited States: The Zincbacteriochlorin−Bacteriochlorin and Bacteriochlorophyll−Spheroidene Complexes *J. Am. Chem. Soc*. **126** 4007; (b) Musib D, Raza M K, Kundu S and Roy M 2018 Modulating In Vitro Photodynamic Activities of Copper(II) Complexes *Eur. J. Inorg. Chem*. **2018** 2011
39. Lin H, Cheng P, Wan C and Wu A 2012 A turn-on and reversible fluorescence sensor for zinc ion *Analyst* **137** 4415
40. Saini A K, Srivastava M, Sharma V, Mishra V and Mobin S M 2016 A highly selective, sensitive and reversible fluorescence chemosensor for Zn^{2+} and its cell viability *Dalton Trans*. **45** 3927
41. Pratibha, Singh S, Sivakumar S and Verma S 2017 Purine-Based Fluorescent Sensors for Imaging Zinc Ions in HeLa Cells *Eur. J. Inorg. Chem*. **36** 4202
42. Huang Z and Lippard S J 2012 Illuminating mobile zinc with fluorescence: From cuvettes to live cells and tissues *Methods Enzymol*. **505** 445
43. Chyan W, Zhang D Y, Lippard S J and Radford R J 2014 Reaction-based fluorescent sensor for investigating mobile Zn^{2+} in mitochondria of healthy versus cancerous prostate cells *Proc. Natl. Acad. Sci. USA* **111** 143